

2016

Study of Role of Meniscus and Viscous Forces During Liquid-Mediated Contacts Separation

Prabin Dhital

Minnesota State University Mankato

Follow this and additional works at: <http://cornerstone.lib.mnsu.edu/etds>



Part of the [Nanoscience and Nanotechnology Commons](#), and the [Tribology Commons](#)

Recommended Citation

Dhital, Prabin, "Study of Role of Meniscus and Viscous Forces During Liquid-Mediated Contacts Separation" (2016). *All Theses, Dissertations, and Other Capstone Projects*. Paper 653.

This Thesis is brought to you for free and open access by the Theses, Dissertations, and Other Capstone Projects at Cornerstone: A Collection of Scholarly and Creative Works for Minnesota State University, Mankato. It has been accepted for inclusion in All Theses, Dissertations, and Other Capstone Projects by an authorized administrator of Cornerstone: A Collection of Scholarly and Creative Works for Minnesota State University, Mankato.

**STUDY OF ROLE OF MENISCUS AND VISCOUS FORCES
DURING LIQUID-MEDIATED CONTACTS SEPARATION**

A thesis submitted in partial fulfillment requirements

For the degree of Master of Science in

Mechanical Engineering

By

Prabin Dhital

MINNESOTA STATE UNIVERSITY, MANKATO

July 2016

The thesis of Prabin Dhital is approved on July 26,2016:

Dr. Shaobiao Cai, PE-Assistant Professor

Date

Dr. Jin Y. Park, Professor

Date

Dr. Kuldeep Agarwal, Assistant Professor

Date

Minnesota State University, Mankato

ABSTRACT

Menisci may form between two solid surfaces with the presence of an ultra-thin liquid film. When the separation operation is needed, meniscus and viscous forces contribute to an adhesion leading stiction, high friction, possibly high wear and potential failure of the contact systems, for instance microdevices, magnetic head disks and diesel fuel injectors. The situation may become more pronounced when the contacting surfaces are ultra-smooth and the normal load is small. Various design parameters, such as contact angle, initial separation height, surface tension and liquid viscosity, have been investigated during liquid-mediated contact separation. However, how the involved forces will change roles for various liquid is of interest and is necessary to be studied.

In this study, meniscus and viscous forces due to water and liquid lubricants during separation of two flat surfaces are studied. Previously established mathematical model for meniscus and viscous forces during flat on flat contact separation is simulated. The effect of meniscus and viscous force on critical meniscus area at which those forces change role is studied with different liquid properties for flat on flat contact surfaces. The roles of the involved forces at various meniscus areas are analyzed. Experiments are done in concerns to studying the effect of surface roughness on contact angle.

The impact of liquid properties, initial separation heights and contact angle on critical meniscus area for different liquid properties are analyzed. The study provides a fundamental understanding of the forces of the separation process and its value for the design of interfaces. The effect of surface roughness and liquid properties on contact angle are studied.

Dedicated to my parents, advisor and friends, I couldn't have done this without you. Thank you
for all of your support along the way.

ACKNOWLEDGMENTS

I express my gratitude and appreciation to my advisor Dr. Shaobiao Cai for his patient guidance, consistent support, encouragement and enthusiasm which allowed me to advance and for providing an optimal environment for conducting research and thanking him for giving me this opportunity to work with him. I would equally like to thank my committee members: Dr. Jin Y Park and Dr. Kuldeep Agrawal for their insightful suggestions and guidance in conducting this research. I would like to thank Mr. Kevin Schull for providing a great environment for accompanying research in the laboratory. Lastly, I would like to thank my parents and friends for their continued support for helping me to achieve my objectives.

TABLE OF CONTENTS

CHAPTER 1	1
1.0 Introduction.....	1
1.1 Research Objectives and Scope	9
CHAPTER 2	10
2.0 Process and Approaches.....	10
2.1 Numerical Modeling	10
2.1.1 Assumptions.....	11
2.1.2 Meniscus Force	11
2.1.3 Viscous Force	13
2.2 Experimental Analysis.....	15
2.2.1 Experimental Setup.....	15
2.2.2 Procedure	19
CHAPTER 3.....	24
3.0 Result and Discussion	24
3.1 Numerical Modelling and Simulation Analysis.....	24
3.2 Experimental Analysis.....	33
3.3 Applications	41
3.4 Conclusion and Suggestion for Future Works	43
4 BIBLIOGRAPHY	46

LIST OF FIGURES

Figure 1.0-1: Schematic of menisci formed between the liquid-mediated contacts [2].	2
Figure 1.0-2: Schematic of meniscus curvature and contact angles at the contact interface of liquid-mediated sphere-on-flat contact [22].	3
Figure 1.0-3: Representation of liquid drop in solid surface.	3
Figure 2.1-1: Formation of liquid bridge with hydrophilic flat on flat liquid-mediated surface contact separation [4] [20].	10
Figure 2.2-1: Carbinet grit paper.	15
Figure 2.2-2: Side View of Instrument (Surface Roughness Tester, TR-200)	16
Figure 2.2-3: Names of each part of the portable roughness measurement device.	17
Figure 2.2-4: Measurement process from surface roughness tester.	17
Figure 2.2-5: Portable surface roughness tester TR200 used for surface roughness measurement of aluminum surface.	18
Figure 2.2-6: Flow diagram of experiment procedure	19
Figure 2.2-7: Wet grinder polisher, Dual Surface.	20
Figure 2.2-8: Experimental arrangements for contact angle measurement.	22
Figure 2.2-9: Simul-Focal microscopy system.	22
Figure 2.2-10: Microscope Digital Camera (10MP APTINA COLOR CMOS ULTRA-FINE COLOR ENGINE INSIDE; MU1000, USB2.0, DC 5V 250mA)	23
Figure 2.2-11: Illustration of contact angle formed on Aluminum surface (Used Grit Paper: 600, Surface Roughness: 0.22 μ m, Liquid: Water).	23
Figure 2.2-12: Illustration of contact angle formed on Aluminum surface (Used Grit Paper: 320, Surface Roughness: 0.59 μ m, Liquid: Castrol Oil).	23

Figure 3.1-1: Relationship between separation height and critical area for various fluid at $\theta_1 = \theta_2 = 60^\circ$ (Room Temperature, 20°) with Separation Time=1s (Note: I; Silicon Oil, II; Glycerol Oil, III; Castrol Oil) [19].....	25
Figure 3.1-2: Dimensional relationship between viscosity and critical meniscus area at contact angles $\theta_1 = \theta_2 = 60^\circ$, Constant γ with 0.0633 N/m (Silicon oil) for separation time =1s, Note: $\eta_0 = 0.4860$ Ns/m ² , Initial meniscus area= 8.50×10^{-10} m ²	28
Figure 3.1-3: Dimensionless relationship between viscosity and critical meniscus area with contact angles $\theta_1 = \theta_2 = 60^\circ$, constant γ with 0.0633 N/m (Silicon oil) for separation time =1s, Note: $\eta_0 = 0.4860$ Ns/m ² , Initial meniscus area= 8.50×10^{-10} m ²	29
Figure 3.1-4: Relationship between initial separation and slope (k) with contact angles $\theta_1 = \theta_2 = 60^\circ$, constant η with .4860 Ns/m ² (Silicon Oil) for separation time=1s, Note: $\gamma_0 = 0.0633$ N/m, Initial meniscus area= 8.50×10^{-10} m ²	29
Figure 3.1-5: Relationship between surface tension and critical area with contact angles $\theta_1 = \theta_2 = 60^\circ$, constant η with .4860 Ns/m ² (Silicon oil) for separation time=1s, Note: $\gamma_0 = 0.0633$ N/m.	30
Figure 3.1-6: Dimensionless surface tension and critical meniscus area with contact angles $\theta_1 = \theta_2 = 60^\circ$, constant η with .4860 Ns/m ² (Silicon oil) for separation time=1s, Note: $\gamma_0 = 0.0633$ N/m, Initial meniscus area= 8.50×10^{-10} m ²	31
Figure 3.1-7: Relationship between meniscus force and critical area with contact Angles $\theta_1 = \theta_2 = 60^\circ$, constant η (0.4860 Ns/m ²) for separation time = 1s, Note: $\gamma_0 = 0.0633$ N/m (silicon oil) [20].	32

Figure 3.1-8: Relationship between meniscus force and critical area with contact angles $\theta_1 = \theta_2 = 60^\circ$, Constant η (0.4860 Ns/m ²) for Separation Time = 1s, Note: $\gamma_o = 0.0633$ N/m (Silicon Oil).	33
Figure 3.2-1: Illustration of different contacts angle during liquid mediated contact separation (600 Grit, water).	39
Figure 3.3-1: Schematic of a data processing magnetic rigid disk drive [21].	41
Figure 3.3-2: Schematic of diesel fuel injector which experiences adhesion [5].	42

LIST OF TABLES

Table 3.1-1:Viscosity and surface tension after increasing with its initial value at room temperature.	28
Table 3.2-1:Roughness parameters of surfaces by using different grit papers.	34
Table 3.2-2:Average value of liquid drops dispensed from the syringe.	34
Table 3.2-3:Contact angle calculation of for different surface roughness (Water).	35
Table 3.2-4:Contact angle calculation for different surface roughness (Castrol Oil).....	35
Table 3.2-5:Contact angle calculation for different surface roughness w.r.t to time (Water).	36
Table 3.2-6:Contact angle calculation for different surface roughness w.r.t to time (Castrol Oil).	37

NOMENCLATURE

F_s	external force, need to overcome the intrinsic forces contributed by meniscus force.
F_m	meniscus force
F_v	viscous force
F_L	the attractive force due to Laplace
F_T	the attractive force due to surface tension
Ω	meniscus area
r_k	kelvin radius
χ_n	meniscus radius
θ	contact angle
$\theta_{1,2}$	the contact angle for the upper surface and the lower surface of the meniscus curve on the upper and the lower contact surfaces
A_{cr}	critical Area
h	separation distance.
r	arbitrary distance
t_s	time to separate
h_s	breakpoint which is infinite during the separation
γ	surface tension
η	viscosity
γ_o	initial surface tension
η_o	initial viscosity
x_c, y_c	center coordinates

CHAPTER 1

1.0 INTRODUCTION

The applications of liquid are common in micro manufacturing to Nanotechnology. Surface contact and friction phenomena are of interest for many of these applications. These applications cover from stress analysis of contact elements and joints, over the influence of lubrication and material design of the friction and wear, to application in micro and nanotechnology. Friction leads to energy dissipation and surface wear during relative motion of contact surfaces. Friction and wear are closely connected with the phenomenon of adhesion so the role of adhesion is essential to many applications [1] . High adhesive force during the separation of two contacting surfaces may cause high friction and stiction and results in high local tensile stresses which may be enough to cause a fracture, generate particles, and delaminate contact surface [1] [2]. As applications of liquids through contact surface are common, the study of the effects of adhesion due the liquid properties is necessary.

When liquid is present at the contact interface of two surfaces, menisci may form around the contacting and near contacting asperities due to surface energy effect of a thin liquid film as shown in Figure 1.0-1. Those formed menisci contribute to adhesion and friction. Increased adhesive force and friction always lead to failure of micro/nanodevices [3]. when liquid-mediated contact is considered, the formed meniscus is the center of interest. The geometric description of the menisci is the meniscus curve which is formed between the upper and lower surfaces of the liquid when the two surfaces come in contact. The shape of this meniscus is determined by the liquid and solid properties. In some surfaces, liquids spread evenly on the surfaces and sometimes it forms into tiny droplets. Hydrophilic liquids spread evenly on the surfaces maximizing contact angle whereas

hydrophobic liquids form a droplet. Formed meniscus is convex for a hydrophobic surface, and concave for a hydrophilic surface. Attractive force (meniscus force) acts on the interference for the hydrophilic surface and repulsive meniscus force acts on the hydrophobic surface [4] [5] [6]. An angle formed between meniscus curve and the contact surface is called contact angle as shown in figures 1.0-2 and 1.0-3. Contact angle can be measured through the important indicator of the contacting system. For a multiphase solid, liquid and gas system under certain conditions (such as different pressures and temperatures), the equilibrium of the system (represented by a unique contact angle) reflects the strength or energy level of the materials. The formation of menisci around the contacting and near contacting surface asperities is due to the effect of the surface energy of the liquid film.

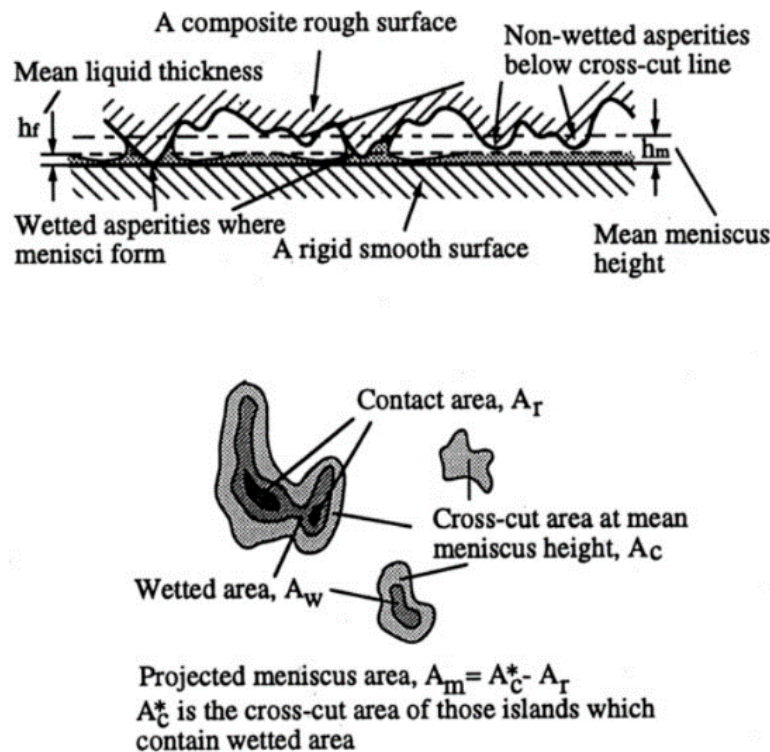


Figure 1.0-1: Schematic of menisci formed between the liquid-mediated contacts [2].

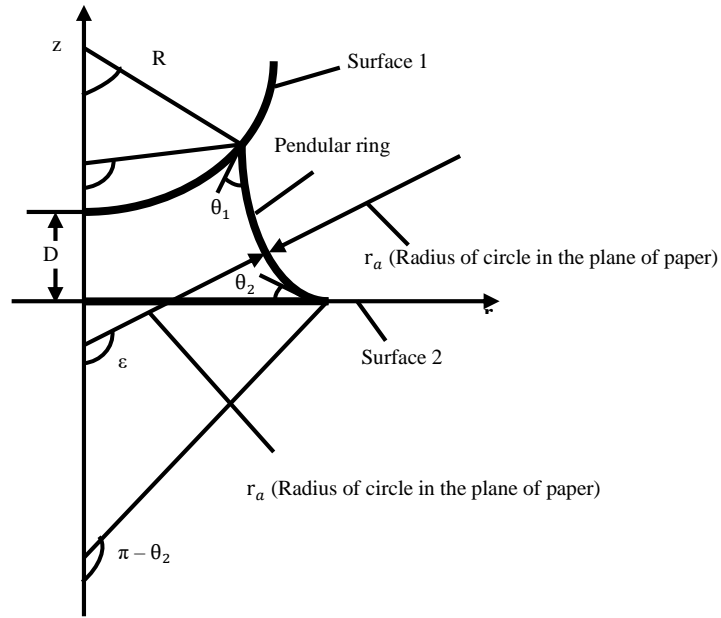


Figure 1.0-2: Schematic of meniscus curvature and contact angles at the contact interface of liquid-mediated sphere-on-flat contact [22].

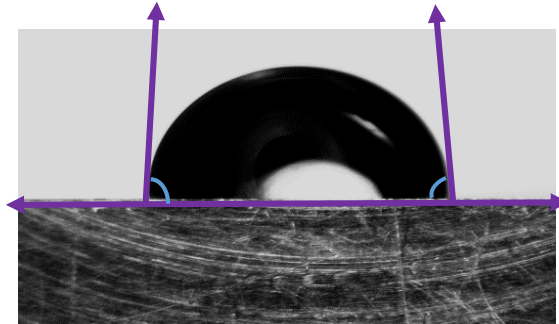


Figure 1.0-3: Representation of liquid drop in solid surface.

Due to start –stop operation, physical contact, sliding phenomenon of devices like magnetic head disks interface, digital micro-mirror devices, and diesel fuel injectors etc. experience adhesion/friction/stiction problems. Various protective coating lubricants are used to provide low friction, low wear, and corrosion resistance. For these protective lubricants, Roles of the meniscus and viscous force involved during liquid-mediated contact surfaces should be analyzed to resolve these problems [5]. Various researches are going on to identify and reduce

adhesion/friction/stiction problems. Adhesion mean the property of different molecules or surfaces to adhere to each other and cohesion mean the property of same molecules of the same substance to stick to each other due to mutual attraction. When two solid surfaces are in contact, adhesion across the interface requires an adhesive force. Adhesion is affected by temperature, surface roughness, and real area of contact, mechanical properties and much more. For example, contacts at high temperature soften the surface resulting in a greater flow of liquid and larger contact area which causes higher adhesion [7]. “Stiction” term was first invented at IBM General Products Division labs at 1980 when they encountered the problem of head slider getting stuck to the disk surface while resting at high humidity due to liquid mediated adhesion [8].

During the liquid-mediated contact separation adhesive bridges or menisci around the contacting and near contacting asperities due to surface energy effect in the presence of a thin liquid film. Liquid-mediated adhesive force during liquid-mediated contact separation can be divided into two components: Meniscus force due to surface tension and a rate dependent viscous force. The viscous component of the adhesive force is significant for more viscous liquids, but it can be dominant for liquids of modest viscosity at high shear rates [9]. During the separation of two surfaces, the viscosity of the liquid causes an additional attractive force, rate dependent viscous force during separation. Meniscus and viscous force cause the break of a meniscus bridge. The resultant force, adhesive or repulsive depends on formed meniscus areas, contact angles, a number of menisci, separation time, and surface tension and viscosity of liquid [2]. Formed menisci between two solid surfaces depend on the surface, either hydrophilic (water loving, formed contact angle is lower than 90°) or hydrophobic (water fearing, formed contact angle is higher than 90°). The meniscus is concave for an interface with hydrophilic surfaces and is convex for hydrophobic surfaces. In hydrophilic surfaces, the attractive meniscus force arises from the negative Laplace pressure inside

the meniscus as a result of surface tension. The product of this pressure difference and the immersed surface area is the adhesive force as a result of liquid-mediated adhesion and denoted as the meniscus force [10].

Surfaces are more complicated than they appear. When the surface of the solid interfaces with the surfaces with liquid, many different results can be observed. For example, solid surfaces can be easily wetted with a high level of adhesion in which case it can be classified as hydrophilic. Liquid drop deposited on a solid surface either spreads or preserves a finite area depending on the interaction of the drop with the solid surface [11]. A liquid drop on the solid surface depends on upon various factors like temperature, surface roughness, properties of the liquid, environmental condition etc. With the increase in surface roughness, there is a decrease in contact angle for hydrophilic surface and increase for hydrophobic surface and there is an increase in contact angle with an increase in surface tension of liquid drops. If the temperature of liquid drop is increased, there is an increase in surface tension, hence the contact angle decreases. [12]. Kittu et al [11] studied the contact angle measurements on a limestone aggregate with different levels of surface roughness and concluded that the magnitude of contact angle decreases as the surface roughness increases.

Meniscus and viscous forces have been believed to be the major contributors to adhesion during separation liquid mediated contact. Many studies have been carried out to study the separation of liquid-mediated contact. Cai and Bushan [4] [5] [6] developed models (CB model) and studied the separation of two flat-on-flat surfaces and sphere-on-flat surfaces. In CB model, various design parameters, such as contact angle, initial separation height, surface tension and liquid viscosity, have been investigated. More importantly, it has been found that the role of involved meniscus force and viscous force changes when so-called critical meniscus area is reached. The behaviors

of a liquid bridge when compressed and stretched in a quasi-static fashion between two solid surfaces that have contact angle hysteresis (CAH) is studied by H.Chen et al [13]. They developed a theoretical model to obtain the profiles of the liquid bridge given a specific separation between the surfaces, where the model is able to correctly predict the behavior of the liquid bridge during a quasi-static compressing/stretching loading cycle in experiments. It has been found that the liquid bridge can have two different profiles at the same separation during one loading and unloading cycle, and more profiles can be obtained during multiple cycles. Kang et al studied the liquid transfer between two separating plates with the aim of increasing the ink transfer ratio in micro gravure offset printing. And the result shows that the liquid transfer ratio increases as the contact angle of a droplet on the lower plate increases and the contact angle on the upper plate decreases. The liquid droplet adheres more strongly to the plate with higher surface energy. This experimental result helps us to determine the optimal surface contact angle [1].

When separation of two liquid mediated contact surfaces is needed, various factors need to be considered in order to characterize the involved forces. The effects of separation distance, initial meniscus height, separation time, and roughness have been studied by S.Cai and B.Bhushan [4] [5]. Contact angle as a one of the major factors in liquid mediated contact has been studied intensively. The study on adhesion contributed by meniscus and viscous forces during the separation of two hydrophilic smooth surfaces with symmetric and asymmetric contact angles were carried out by Cai and Bhushan [2] [5]. In the study, a critical meniscus area was first identified and defined as the meniscus area at which meniscus and viscous forces change role. It was found that with the increase in separation distance, meniscus forces decrease and the integrative viscous force needed to overcome increases. The increase in initial meniscus height for rough surfaces and the increase in surface roughness increases in meniscus force have a significant effect on the

viscous force [5]. L.Wang et al [14] investigated a dynamic separation process of a sphere from a flat and sphere from sphere with an intervening liquid meniscus under constant applied force, for each case the meniscus and viscous force are considered to account for the adhesion force in the separation processes and compared with the dominated adhesion force in the process. And it has been found that the separation time is longer for sphere-on-sphere for same limitations. Popov [15] studied the stick-slip behavior of liquid-mediated contacts. It was observed that the mechanical properties of the liquid menisci changed the amplitude and period of the stick-slip phenomena, which indicated that substantial change may occur depending on the size and properties of the liquid meniscus. Since adhesion has a significant effect on the operation accuracy of devices like MEMS/NEMS, it should treat carefully [16] [17].

For the separation of two surfaces with formed liquid bridge, an external force larger than the meniscus force is required to initiate the separation process, and higher level force may be needed to overcome the additional viscous contribution thereafter. It is noticed that meniscus force continually decreases whereas the integrated viscous over the separation distance from the initial position increases. This indicated the role of the meniscus and viscous force may be changed during the separation process. This has been numerically proved through the simulation of separation process [4]. Further, the effects of separation distance, initial meniscus height, separation time, contact angle, division of menisci and roughness on the meniscus and viscous force were analyzed in the study. The results showed that the viscous force increases with an increase in separation distance. Initial meniscus height is also one of the major factors which affect the magnitude of viscous force during separation process where viscous force decreases with increase in initial meniscus height. Time taken to break meniscus during separation process is the separation time. It is common that separation time is less than a second or in about microsecond

scale. The longer the separation time, the smaller the magnitude of the viscous force since the viscous force during the separation process is inversely proportional to the separation time [2] [4] [5]. Meniscus force contributes to an intrinsic adhesion due to the formed menisci. During the separation of contact surfaces, the viscosity of the liquid causes an additional attractive force, a rate dependent viscous force. Both meniscus and viscous force cause an adhesive force during the separation. During the surface contact and when separation operation of two contact surfaces is needed, adhesion due to the meniscus and viscous force is one of the major reliability issues leading to reduction in the consistency of diesel fuel injectors and micro-mirror devices that experience adhesion. The issue becomes more severe when the applied load is small (which is common) for micro or nanoparticle devices. The force required to separate two surfaces depends on the total force of both meniscus and viscous forces. It has been found that this type of adhesive force is highly dependent on the formed meniscus area, separation time, and surface tension and viscosity of the liquid. Meniscus force continually decreases whereas the integrated viscous (to be overcome) over the separation distance from the initial position increases during the separation process. The role of the two forces changes from meniscus to viscous force before the surfaces are separated.

Although the effects on the meniscus and viscous contributed adhesion during separation of liquid-mediated contact have been studied, the role changes of the contributed forces are not adequately investigated. It is known that a critical meniscus area determines the role change of the forces. However, questions like how does the critical meniscus area change with the change of the affecting factors, such as liquid properties, need to be answered in order to effectively solve the adhesion caused issues.

1.1 RESEARCH OBJECTIVES AND SCOPE

Adhesion, friction, stiction, and wear are the main issues in applications like magnetic head disks, micro-devices, diesel fuel injectors etc. during liquid-mediated contact separation. These issues are associated with contact configuration of two surfaces, surfaces roughness, properties of used liquid, and meniscus and viscous forces of liquid-mediated contact separation. The purpose of this study is to understand the effect of liquid properties on viscous and meniscus force, the roles of adhesive forces due to separation from liquid menisci during flat on flat liquid-mediated contact separation.

The effect of the meniscus and viscous forces on critical meniscus area at which those forces change the role is studied with different liquid properties for flat on flat contact surfaces separation. And previously established mathematical model of the meniscus and viscous forces for flat on flat liquid-mediated contact separation is simulated and data analysis is performed. The experimental analysis is made in order to examine the effect of roughness on contact angle with a different liquid.

CHAPTER 2

2.0 PROCESS AND APPROACHES

The research is achieved by two different ways, first of all Numerical modeling (Mainly) is performed in order to study the roles of meniscus and viscous forces during flat on flat liquid-mediated contacts separation and secondly, experimental analysis is made in order to analyses the effect of surface roughness on contact angle for different liquid properties.

2.1 NUMERICAL MODELING

As part of data collection procedure, already established mathematical model is simulated on MATLAB to analyze the roles of the meniscus and viscous force with different liquid properties for various liquids, such as water and commonly used liquid lubricants like Silicon oil, Castrol oil, and Glycerol. Figure 2.1-1 shows the configuration of the meniscus formed between flat on flat contact surfaces.

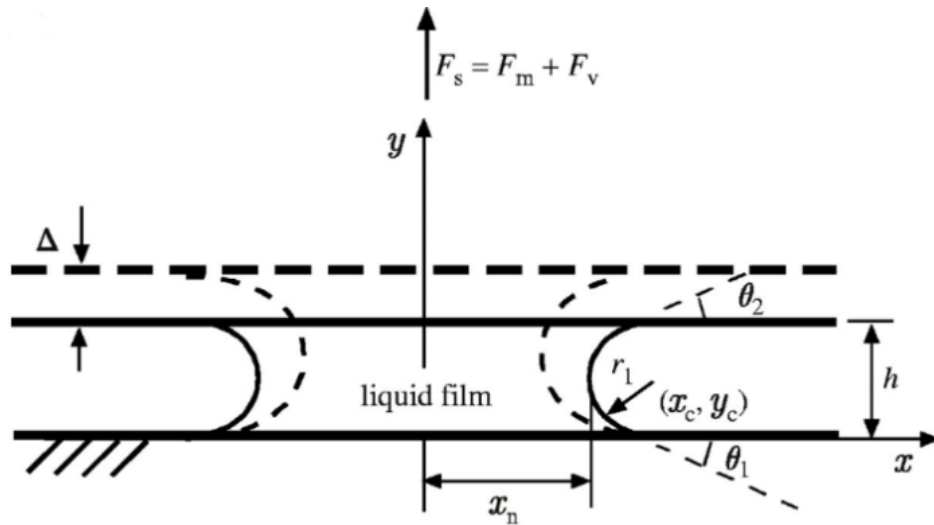


Figure 2.1-1: Formation of liquid bridge with hydrophilic flat on flat liquid-mediated surface contact separation [4] [20].

2.1.1 Assumptions

The two contact surfaces are assumed as rigid. The formed meniscus bridge is considered to be mechanical equilibrium and used liquid is incompressible with no thermal effect. The pressure is constant on a vertical cross section plane, whereas it varies along a radial direction through the meniscus bridge during the process of separation. An arc-shaped meniscus is supposed.

2.1.2 Meniscus Force

Meniscus forming between the two flat surfaces due to a surface tension γ resulting in pressure difference Δp (which is often referred to as capillary pressure or Laplace pressure) is given by the Laplace equation.

$$\Delta p = \gamma \left(\frac{1}{r_1} + \frac{1}{r_2} \right) \quad (1)$$

Where, r_1 is the meniscus radius and r_2 is another radius of the meniscus in the orthogonal plane to the plane r_1 belonging to (not shown in Figure 2-1.1).

It is noticed that one may neglect the surface tension contribution when the initial meniscus neck radius $x_0 \gg r_1$ is true. If $r_2 \gg r_1$ does not hold, r_2 may be replaced with the difference between x_c , the center coordinate of the meniscus curve, and r_1 . Thus, $r_2 \rightarrow x_c - r_1$.

The meniscus force on flat on flat contact due to the formation of a meniscus is obtained by integrating the Laplace pressure over the meniscus area and adding the surface tension effect acting on the circumference of the interface [18].

$$F_m = F_L + F_T \quad (2)$$

$$F_m = \iint_{\Omega} \Delta p d\Omega + 2\pi\gamma\chi_n \sin \theta_{1,2} \quad (3)$$

$$F_m = \pi \chi_n^2 \frac{\gamma}{r_k} + 2\pi \gamma \chi_n \sin \theta_{1,2} \quad (4)$$

Where,

F_s is the external force which is needed to overcome the intrinsic forces contributed by meniscus force.

F_m is the meniscus force.

F_v is the viscous force.

F_L is the attractive force due to Laplace.

F_T is the attractive force due to surface tension.

h is the separation height.

γ is the liquid surface tension.

r_k is the kelvin radius.

Ω is the meniscus area.

χ_n is the meniscus radius.

θ is the contact angle between the solid surfaces with the as upper surface and the lower surface of the formed meniscus.

$\theta_{1,2}$ is the contact angle for the upper surface and the lower surface for the meniscus curve on the upper and the lower contact surfaces.

x_c, y_c are the center coordinates.

The meniscus height is calculated using the following expression:

$$h = r_k (\cos \theta_1 + \cos \theta_2) \quad (5)$$

The meniscus force in terms of separation height is given by:

$$F_m = \frac{\pi \chi_n^2 \gamma (\cos \theta_1 + \cos \theta_2)}{h} + 2\pi \gamma \chi_n \sin \theta_{1,2} \quad (6)$$

And meniscus neck radius can be expressed as equation (7)

$$x_n = x_c - r_1 \sin \theta_{1,2} \quad (7)$$

2.1.3 Viscous Force

Viscous force occurs due to the viscosity of the liquid when two surfaces are separated within a short time. Characterization of the viscous force is important in order to estimate the total force needed to separate two liquid-mediated contact surfaces. The equation for the viscous force during the separation of flat on flat surfaces has been derived by using Reynolds lubrication equation with a cylinder coordinate system [18].

$$\frac{\partial}{\partial r} \left(r h^3 \frac{\partial p}{\partial r} \right) = 12 \eta r \frac{dh}{dt} \quad (8)$$

Where h is the separation distance and r is an arbitrary distance in the central plane of the meniscus in the direction of separation.

The pressure difference in and outside the meniscus can be found by integrating the lubrication equation.

$$\Delta p = \frac{3\eta}{h^3} (r^2 - x_n^2) \frac{dh}{dt} \quad (9)$$

The average pressure difference between the center and the outside boundary of the meniscus which can be found as:

$$\Delta p_{avg} = -\frac{3\eta}{2h^3} x_n^2 \frac{dh}{dt} \quad (10)$$

For the separation of two smooth flat surfaces, the viscous force during the separation of two flat on flat surfaces at given separation height is:

$$F_v = \frac{3\pi\eta\chi_{ni}^4}{4t_s} \left(\frac{1}{h_s^2} - \frac{1}{h_0^2} \right) \quad (11)$$

Where t_s the time to separate two surfaces is, h_s is the break point which is infinite during the separation, and h_0 is the initial gap between the two flat surfaces.

Both the meniscus and viscous force operate inside the meniscus during the separation process in surface contact. So the conditions like asymmetric angles, division meniscus, separation time and height can significantly affect the properties of the meniscus and viscous force during separation. An external force is required to initiate the separation process. During the break point, external force should be larger than a total of the meniscus and viscous force. Through the contact of the two liquid-mediated surfaces, if the meniscus force is larger than that of the viscous force, the meniscus will break slowly without the application of external forces, however, the time to separate is longer.

2.2 EXPERIMENTAL ANALYSIS

Experimental analysis is performing in order to investigate the effect of different surface roughness with different liquid properties (water and Castrol Oil) at room temperature.

2.2.1 Experimental Setup

In addition to analyzing the effect of surface roughness on contact angle, different surface finishing grits (*Refer to Figure 2.2-1*) are used to varied roughness. And a drop of liquid under investigation is placed between the two surfaces. The formed meniscus is captured and the contact angle is determined by using AMSCOPE.



Figure 2.2-1: Carbimet grit paper.

Measuring Principle of TR-200 Surface Roughness Tester

TR-200 portable roughness instrument applies (*Refers to Figures 2.2-2 & 2.2-3*) to production site and can be used to measure surface roughnesses of various machinery-processed parts, calculate corresponding parameters according to selected measuring environments and visibly display all

measurement parameters and profile graphs on LCD and its include features are as below (*Shown in Figure 2.2-4*):

- Multiple parameter measurements: Ra, Rz, Ry, Rq, Rp, Rm, Rt, R3z, Rmax, Sk, S, Sm, and tp;
- Highly sophisticated inductance sensor;
- Four-wave filtering methods of RC, PR-RC, GAUSS, and D-P;
- Compatible with four standards of ISO, DIN, ANSI and JIS;
- 128 × 64 lattice LCD displays all parameters and graphs;
- DSP chip is used to control and process data with high speed and low power consumption;
- Built-in lithium ion chargeable battery and control circuit with high capacity, without memory effect with consecutive work time is longer than 20 hours;
- Design of mechanical and electrical integration is adopted to achieve small bulk, light weight, and easy usage;
- Automatic switch off, memory and various prompt instructions;

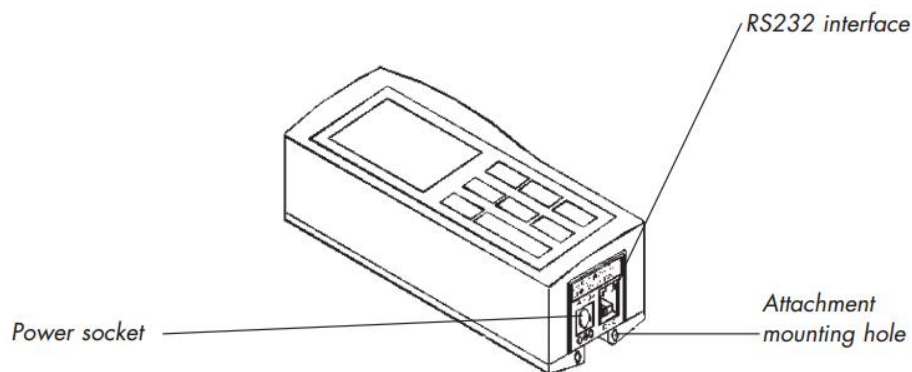


Figure 2.2-2: Side View of Instrument (Surface Roughness Tester, TR-200)

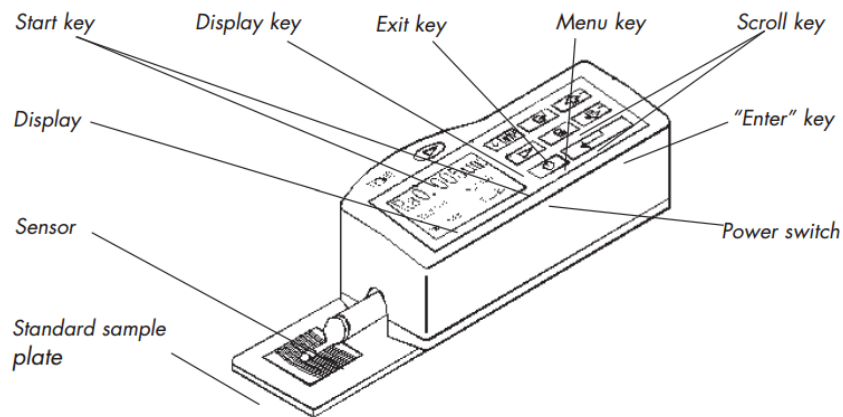
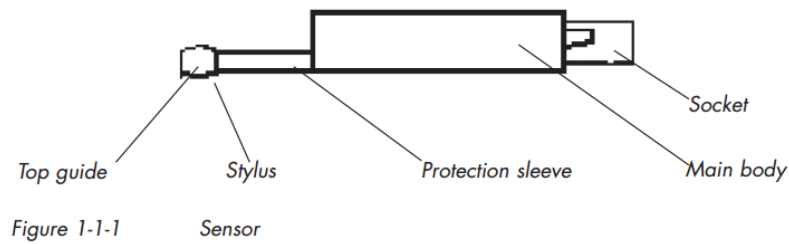


Figure 2.2-3: Names of each part of the portable roughness measurement device.

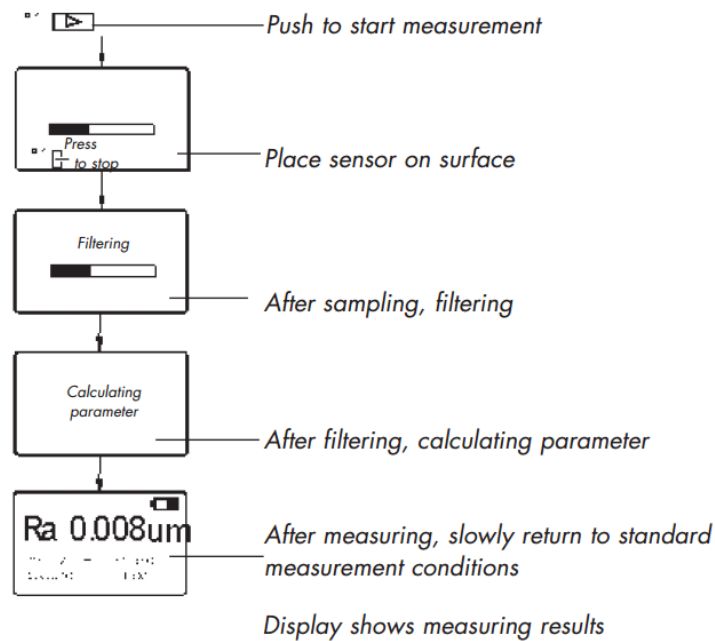


Figure 2.2-4: Measurement process from surface roughness tester

In order to measure the surface roughness of specified surfaces, initially, the sensor is placed on the surface and then it is uniformly slid along the surface. The sensor gets surface roughness by sharp built-in-probe. This roughness causes displacement of the probe which results in a change of the inductive amount of induction coils so as to generate an analog signal, which is in proportion to surface roughness at the output end of the phase-sensitive rectifier. After amplification and level conversion this signal enters the data collection system. After that, those collected data are processed with digital filtering and parameter calculation by DSP chip. The measurement results are displayed by LCD screen as shown in Figure 2.2-5.



Figure 2.2-5: Portable surface roughness tester TR200 used for surface roughness measurement of aluminum surface.

2.2.2 Procedure

The flow diagram of experimental analysis is shown in figure below:

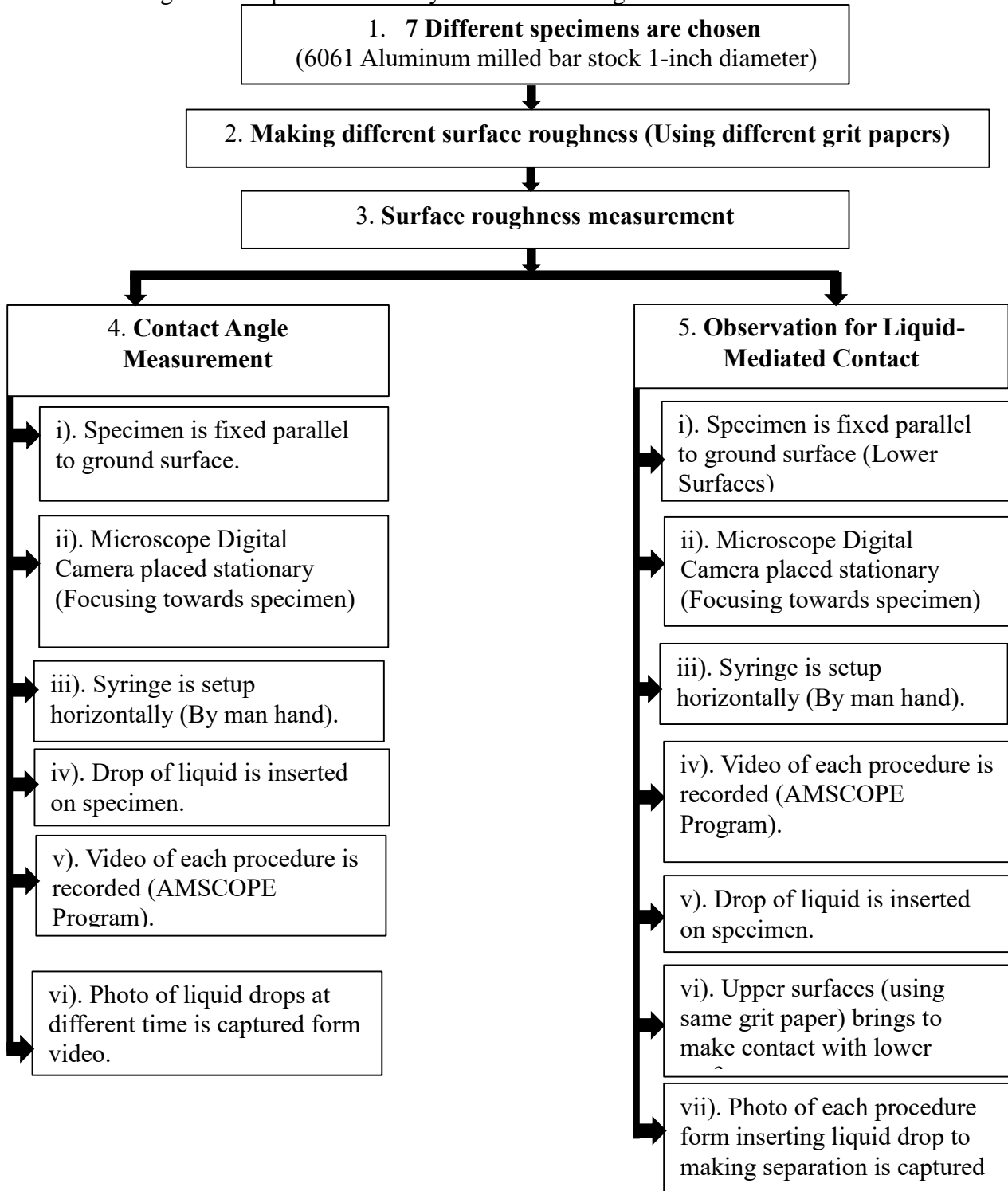


Figure 2.2-6: Flow diagram of experiment procedure



Figure 2.2-7: Wet grinder polisher, Dual Surface.

To determine the effect of surface roughness on contact angle, initially, 7 different flat 6061 Aluminum (milled bar stock 1-inch diameter) specimens are taken as sample preparation. Each specimen surface is ground using different grit (180,320,400 &600) paper shown in figure 2.2-7 in order to get different surface roughness. The surface roughness of each sample is measured by portable surface roughness tester as shown in figure 2.2-5 above. The surface of each sample is rubbed with alcohol before liquid drop is poured. Each sample is placed parallel to the ground surface and then fixed in a vice. A vertically projected syringe is fixed to pour the liquid drop on the surface. Every time a drop of liquid is dispensed vertically from the syringe, which is capture in video mode. Figure 2.2-6 and 2.2-8 shows the contact angle measurement facility. A vice is used to fix the aluminum surfaces. A drop of liquid is dispensed vertically from the syringe and a light source is arranged in order to illuminate the drop of liquid clear from opposite side of microscope lens. Each drop of liquid is captured in video by the microscope (Figure 2.2-9 and

2.2-10) and displayed by AMSCOPE Software. Picture of liquid drops is captured from the video mode at the different time and the contact angle of each drop is determined by using geometric line function of AMSCOPE Software shown in figures 2.2-11 and 2.2-12 below. To determine the contact angle of liquid, first of all, a horizontal line is drawn at the base of a liquid drop and two tangent line are outlined on the curve made formed by liquid drop with baseline. After the measurement of two contact angle form the drop, the overall contact angle form is taken as an average between two angles. Finally, the relationships between the contact angles with surface roughness, the effect of liquid properties on contact angle are analyzed.

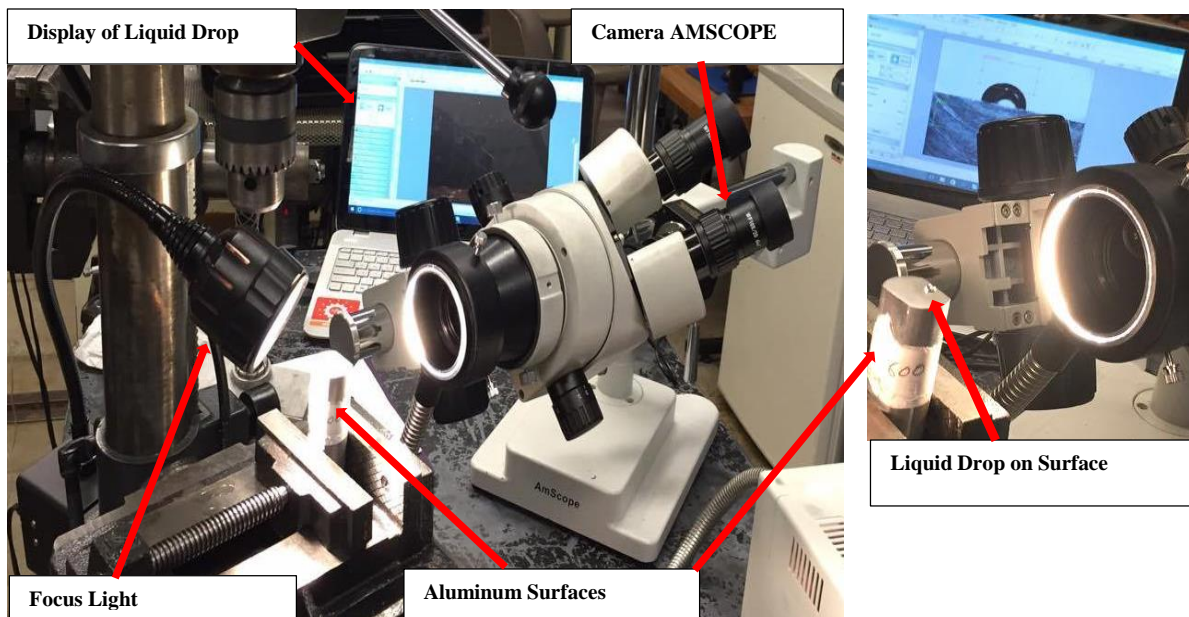


Figure 2.2-8: Experimental arrangements for contact angle measurement.



Figure 2.2-9: Simul-Focal microscopy system.



Figure 2.2-10: Microscope Digital Camera (10MP APTINA COLOR CMOS ULTRA-FINE COLOR ENGINE INSIDE; MU1000, USB2.0, DC 5V 250mA)



Figure 2.2-11: Illustration of contact angle formed on Aluminum surface (Used Grit Paper: 600, Surface Roughness: $0.22\mu\text{m}$, Liquid: Water).



Figure 2.2-12: Illustration of contact angle formed on Aluminum surface (Used Grit Paper: 320, Surface Roughness: $0.59\mu\text{m}$, Liquid: Castrol Oil).

CHAPTER 3

3.0 RESULT AND DISCUSSION

Two flat on flat on liquid-mediated contact surfaces are separated from a liquid meniscus in order to perform simulation analysis. Meniscus and viscous forces are calculated during separation based on various initial meniscus heights from 2 nm to 6nm. Critical meniscus area (at which meniscus and viscous force change roles, i.e. meniscus and viscous force may dominate each other) is calculated at each separation height. Initially, three different liquids, silicon oil, glycerol oil and Castrol oil are taken. And the experimental analysis is performed in order to demonstrate the feasibility study of surface roughness on contact angle and the observation analysis during liquid-mediated contact separation

3.1 NUMERICAL MODELLING AND SIMULATION ANALYSIS

The meniscus and viscous forces play a role during liquid-mediated contact separation. Depending on the size of meniscus area, either of them can be the dominant force. The meniscus area at which meniscus or viscous force changes roles is called critical meniscus area. The meniscus force is dominant one if meniscus area is smaller than critical meniscus area; otherwise, the viscous force is a dominating force. The study showed that critical meniscus area changes with an initial separation of two flat surfaces and liquid properties (surface tension and viscosity) as shown in Figure 3.1-1 below. Three lubricant liquids, silicon oil, glycerol oil and Castrol oil, are used in order to analyze. It is observed from Figure 3.1-1 that critical meniscus area increases with the increase in initial separation distance of the flat surfaces for a specific lubricant. This indicates that at larger initial separation, a large meniscus size is needed for the viscous force to be the dominate

force. Meniscus force will be the one need to be handled if the size of meniscus is limited within the critical meniscus area

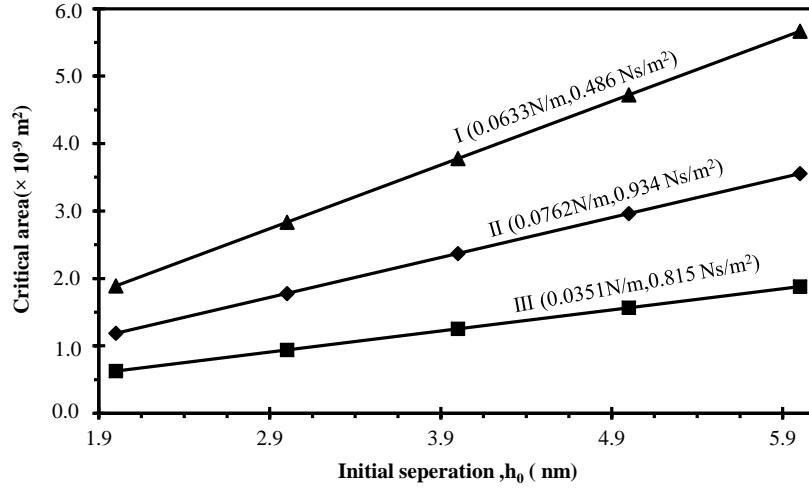


Figure 3.1-1: Relationship between separation height and critical area for various fluid at $\theta_1 = \theta_2 = 60^\circ$ (Room Temperature, 20°) with Separation Time=1s (Note: I; Silicon Oil, II; Glycerol Oil, III; Castrol Oil) [19].

In order to establish the relation between viscosity and surface tension with critical meniscus area at which the force change role, the analysis is performed for silicon oil at room temperature with viscosity value of 0.0633 N/m, the surface tension of 0.4860 Ns/m² and separation time of 1 second with a contact angle of 60°. Initially, preliminary liquid properties value of viscosity and surface tension at room temperature are inserted in the equations 4 and 6 during flat on flat separation which is programmed on MATLAB. The resulting critical meniscus area, and meniscus and viscous force values are recorded. The simulated equation gives the values of critical meniscus area at different heights (2nm to 6nm) for corresponding meniscus and viscous forces for different liquid properties. Every time when the different liquid properties value is inserted, simulated program gives the corresponding value of meniscus and viscous forces, and critical meniscus area which is noted for further analysis.

Thus the symbols ● ■ ▲ ◆ and ○ represent the critical meniscus area values with different viscosity and surface tension for initial meniscus height from 2nm to 6nm respectively and highlighted dashes box on left side of graph represent the initial critical meniscus area for different initial meniscus height for silicon oil ($\eta_0=0.4860 \text{ Ns/m}^2$ and $\gamma= 0.0633 \text{ N/m}$) at room temperature during flat on flat liquid mediated contact separation (*Refers to Figures 3.1-2, 3.1-3, 3.1-4, 3.1-5, 3.1-6, & 3.1-7*). After the critical meniscus area at room temperature is recorded, viscosity value is theoretically increased by 5%, 10%, 15%, 20%, 25%, 30%, 35%, 40%, 50%, and 100% (*Refer to Figures 3.1-2, & 3.1-3*) of its initial value, keeping the surface tension value constant (0.0633 N/m) and secondly, surface tension value is theoretically increased by 5%, 10% ,15%, 20%, 25%, 30%, 35%, 40%, 50%, and 100% (*Refer to Figure 3.1-5, & 3.1-6*) of its initial value keeping the viscosity value constant (0.4860 Ns/m²). In order to study the effect of viscosity, initial value of liquid properties is taken as silicon oil ($\eta_0=0.4860 \text{ Ns/m}^2$ and $\gamma= 0.0633 \text{ N/m}$). The initial value of surface tension is kept constant as 0.0633N/m while the viscosity value is increased by 5%, 10%, and so on with its initial value. Every time the constant surface tension value (0.0633N/m) and result through increased in viscosity value are inserted on the simulated program. For example, increased by 5% of initial viscosity is 0.510 Ns/m², 10% of initial viscosity is 0.535 Ns/m², hence the new liquid properties 0.0633N/m and 0.510Ns/m², 0.0633N/m and 0.535 Ns/m² and so on are inserted on program separately. And to analyze the effect of surface tension, initial value of liquid properties is also taken as silicon oil ($\eta_0=0.4860 \text{ Ns/m}^2$ and $\gamma= 0.0633 \text{ N/m}$). The initial value of viscosity is kept constant as 0.4860 Ns/m² however the surface tension value is increased by 5% ,10% and so on with its initial value. Every time the constant viscosity value (0.4860 Ns/m²) and result by increased surface tension value are inserted on the simulated program. For example, increased by 5% of initial surface tension is 0.0665 N/m, 10% of initial viscosity is 0.0696 N/m,

hence the new liquid properties 0.0665N/m and 0.4860Ns/m^2 , 0.0696N/m and 0.4860Ns/m^2 and so on are inserted on program separately. Table 3.1-1 shows the corresponding increased value of viscosity and surface tension with its initial. This different viscosity and surface tension values are inserted into the program with flat on flat viscous force calculation and the critical meniscus area are recorded for different initial heights. Figures 3.1-2 and 3.1-3 shows the increasing viscosity and Figures 3.1-5 and 3.1-6 shows increasing surface tension value from left to right on the x-axis and corresponding critical meniscus area on the y-axis.

After the analysis with increasing viscosity and using constant surface tension, Figures 3.1-2 and 3.1-3 summarizes the effect of liquid viscosity on critical meniscus area during flat on flat liquid-mediated contact separation. It is observed that initial meniscus height and viscosity of liquid have a significant effect on critical meniscus area. The results show that with the contact angles of Θ_1 and Θ_2 as 60° , an increase in initial meniscus height leads to a larger critical meniscus area for same viscosity. This is because a larger initial meniscus height leads to a much faster decrease in viscous force compared to the meniscus force so a larger meniscus area is needed for the viscous force to become comparable to meniscus force. The ratio of increase of critical meniscus area for increasing viscosity are always same for 2nm to 3nm, 3nm to 4nm, 4nm to 5nm and 5nm to 6nm separation heights. The result shows that changing of the critical area from 5nm to 6nm has a higher ratio and followed by 4nm to 5nm, 3nm to 4nm and 2nm to 3nm presented on Figure 3.1-4 as slope analysis. Also, it is observed that critical meniscus area moves to a smaller value with increase in viscosity. The decrease in critical meniscus area will result in a decrease in meniscus force. From the Figure.3.1-2, we can also observe that change in critical area from 2nm to 6nm initial separation is about constant as viscosity increases.

Table 3.1-1:Viscosity and surface tension after increasing with its initial value at room temperature.

Initial Viscosity and Surface Tension at Room Temperature for Silicon Oil	$\eta_o = 0.4860 \text{ Ns/m}^2$	$\gamma_o = 0.0633 \text{ N/m}$
Increased Percentage with Initial value	Viscosity (Ns/m ²)	Surface tension (N/m)
5%	0.5100	0.0665
10%	0.5350	0.0696
15%	0.5590	0.0728
20%	0.5830	0.0760
25%	0.6080	0.0791
30%	0.6320	0.0823
35%	0.6560	0.0855
40%	0.6800	0.0886
50%	0.7290	0.0950
100%	0.9720	0.1266

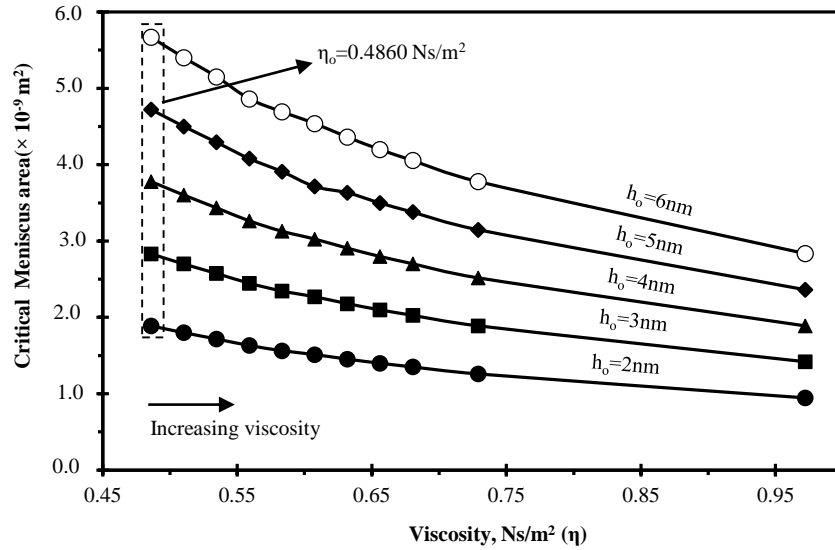


Figure 3.1-2: Dimensional relationship between viscosity and critical meniscus area at contact angles $\theta_1 = \theta_2 = 60^\circ$, Constant γ with 0.0633 N/m (Silicon oil) for separation time =1s, Note: $\eta_o = 0.4860 \text{ Ns/m}^2$, Initial meniscus area= $8.50 \times 10^{-10} \text{ m}^2$.

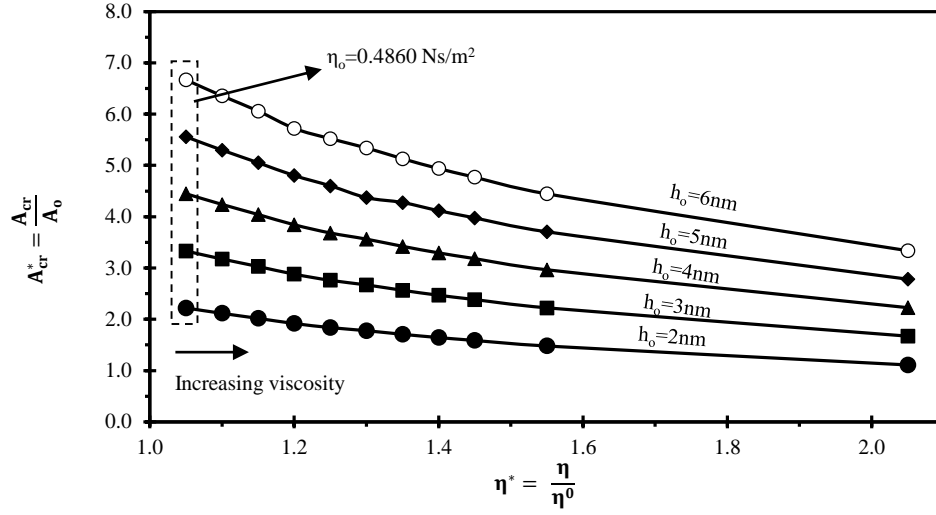


Figure 3.1-3: Dimensionless relationship between viscosity and critical meniscus area with contact angles $\theta_1 = \theta_2 = 60^\circ$, constant γ with 0.0633 N/m (Silicon oil) for separation time = 1s, Note: $\eta_0 = 0.4860 \text{ Ns/m}^2$, Initial meniscus area = $8.50 \times 10^{-10} \text{ m}^2$.

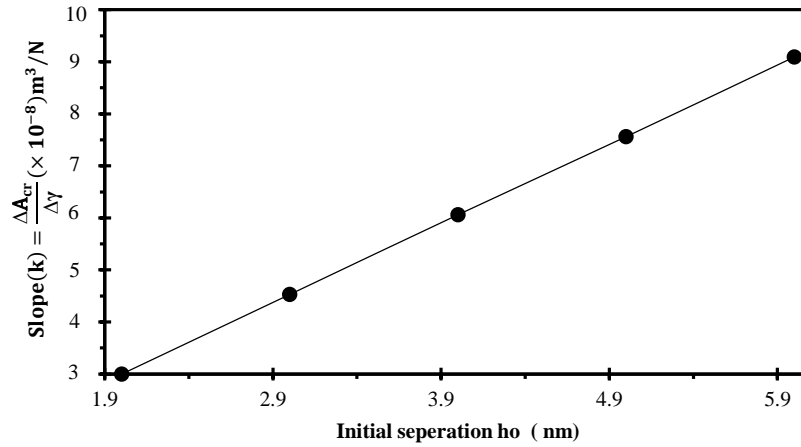


Figure 3.1-4: Relationship between initial separation and slope (k) with contact angles $\theta_1 = \theta_2 = 60^\circ$, constant η with 0.4860 Ns/m² (Silicon Oil) for separation time = 1s, Note: $\gamma_0 = 0.0633 \text{ N/m}$, Initial meniscus area = $8.50 \times 10^{-10} \text{ m}^2$.

When the viscosity of the liquid is kept constant and surface tension value is increases, Figures 3.1-5 & 3.1-6 review the effect of liquid surface tension on critical meniscus area during flat on flat liquid-mediated contact separation. It is observed that initial meniscus height and surface tension of liquid have a significant effect on critical meniscus area. The results also show that with

contact angles of Θ_1 and Θ_2 as 60° , an increase in initial meniscus height leads to a larger critical meniscus area for same surface tension. This is because a larger initial meniscus height leads to a much faster decrease in viscous force compared to meniscus force so a larger meniscus area is needed for the viscous force to become comparable to meniscus force. The ratio of increase of critical meniscus area for increasing surface tension is also always same for 2nm to 3nm, 3nm to 4nm, 4nm to 5nm and 5nm to 6nm separation heights. The result shows that changing of critical meniscus area ratio from 5nm to 6nm has higher value followed by 4nm to 5nm, 3nm to 4nm and 2nm to 3nm, same as for the role of viscosity analysis on Figures 3.1-2 & 3.1-3. It is observed that critical meniscus area moves to a higher value with increase in surface tension. From Figure 3.1- we can also conclude that the change in the critical area from 2nm to 6nm initial separation is constant as surface tension increases.

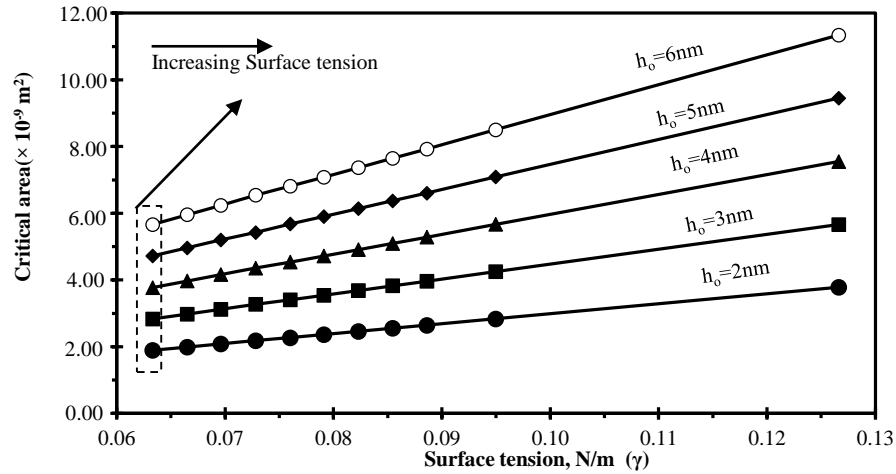


Figure 3.1-5: Relationship between surface tension and critical area with contact angles $\Theta_1 = \Theta_2 = 60^\circ$, constant η with .4860 Ns/m² (Silicon oil) for separation time=1s, Note: $\gamma_0 = 0.0633$ N/m.

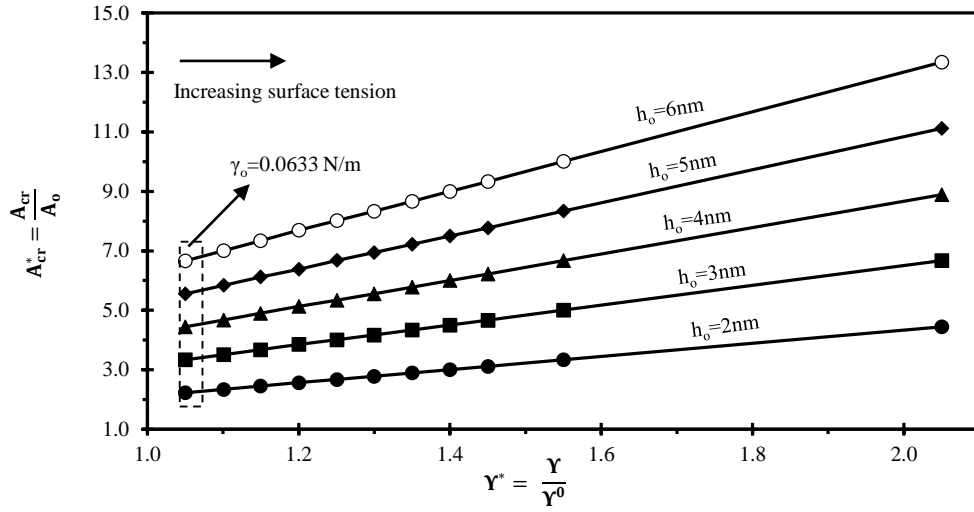


Figure 3.1-6: Dimensionless surface tension and critical meniscus area with contact angles $\theta_1 = \theta_2 = 60^\circ$, constant η with 4860 Ns/m^2 (Silicon oil) for separation time = 1s, Note: $\gamma_0 = 0.0633 \text{ N/m}$, Initial meniscus area = $8.50 \times 10^{-10} \text{ m}^2$.

The relationship between the meniscus and viscous forces with critical meniscus area with relation to viscosity and separation height is shown in Figure 3.1-7. It is observed that critical meniscus area decreases with increase in liquid viscosity for the cases that surface tension is constant with constant initial meniscus height. This is due to a more rapid increase in viscous force when the viscosity of the liquid is higher. Thus viscous force can dominate at smaller critical meniscus area. It is also noticed that lower initial meniscus height has a smaller critical meniscus area. In addition, the rate decrease in critical meniscus area is also smaller for a lower initial meniscus height when the liquid viscosity is increased [20].

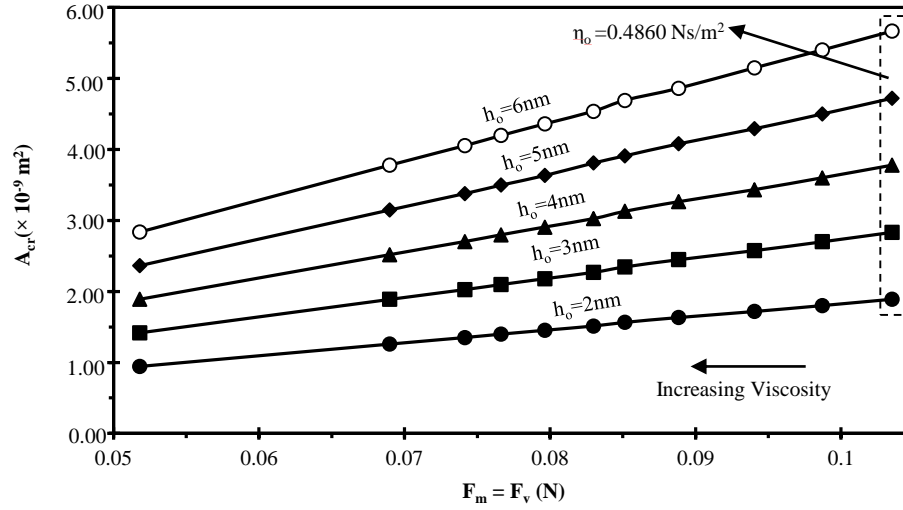


Figure 3.1-7: Relationship between meniscus force and critical area with contact Angles $\theta_1 = \theta_2 = 60^\circ$, constant η (0.4860 Ns/m^2) for separation time = 1s, Note: $\gamma_o = 0.0633 \text{ N/m}$ (silicon oil) [20].

The relationship between the meniscus and viscous forces with critical meniscus area with relation to surface tension and separation height is present on Figure 3.1-8. It shows the effect of initial meniscus height and surface tension to critical meniscus area in a dimensional analysis. It is observed that for a constant initial meniscus height, critical meniscus area (at which meniscus force equals the viscous force) increases with increase in liquid surface tension. The lower initial meniscus height has a smaller critical meniscus area. In addition, the rate increase in critical meniscus area is also smaller for a lower initial meniscus height. This confirms the observation made previously. These observations indicate that viscous force may be likely to take a dominant role when initial meniscus height is smaller.

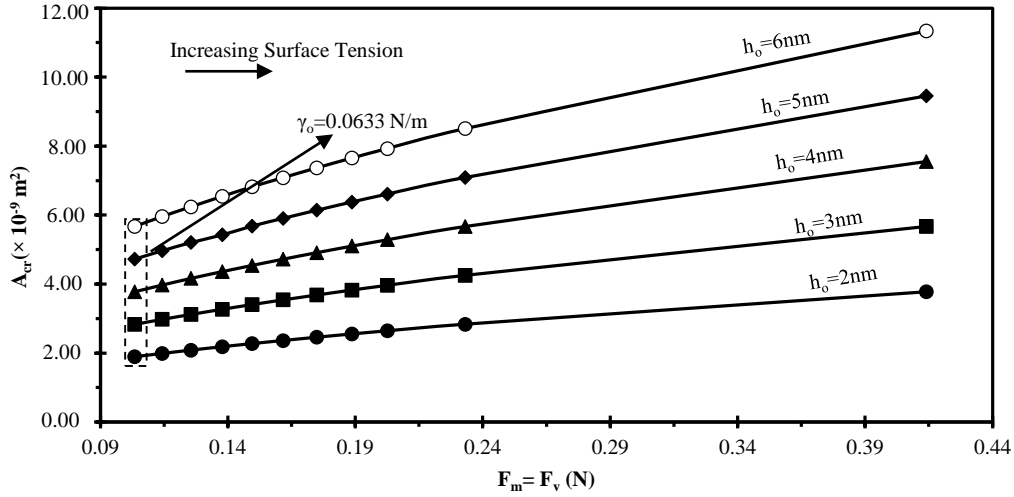


Figure 3.1-8: Relationship between meniscus force and critical area with contact angles $\theta_1 = \theta_2 = 60^\circ$, Constant η (0.4860 Ns/m^2) for Separation Time = 1s, Note: $\gamma_o = 0.0633 \text{ N/m}$ (Silicon Oil).

The results (figures 3.1-1 to 3.1-8) from numerical modelling simulation analysis can be used as the liquid properties selection model chart for a specific critical meniscus area and separation height for micro-nano device applications.

3.2 EXPERIMENTAL ANALYSIS

In order to demonstrate the feasibility study of surface roughness on contact angle, all samples are chosen as aluminum. The surfaces of all each specimen have same surface energy because all of them are polished by same polishing powder. The average roughness values of the specimen are made different by using different grit papers which are shown in Table 3.2-1.

Table 3.2-1: Roughness parameters of surfaces by using different grit papers.

Sample	Grit Papers	Roughness(μm)
1	600	0.220
2	600	0.359
3	400	0.434
4	400	0.470
5	320	0.499
6	320	0.559
7	180	0.590

Each of the specimens is fixed on vice and surface is balanced by using the liquid level meter. A drop of liquid is dispensed vertically from the syringe. Table 3.2-2 shows the average volume of each drop dispensed from the syringe for water and Castrol oil.

Table 3.2-2: Average value of liquid drops dispensed from the syringe.

	Water	Castrol Oil
Sample	Weight (grams)	Weight(grams)
1	0.01150	0.00770
2	0.01120	0.01020
3	0.01300	0.00970
4	0.01450	0.01030
5	0.01300	0.01080
6	0.01280	0.01060
7	0.01360	0.00970
8	0.01120	0.01050
9	0.01320	0.01050
10	0.01390	0.01060
Average	0.01279	0.01006

Each drop of the liquid dispensed from the syringe is captured by using Camera (AMSCOPE) in the video mode. A drop of liquid on the surface after dispensing from the syringe is captured from video mode and the contact angle of liquid drop is determined by using AMSCOPE software. Contact angles for different roughness are shown in Table 3.2-3 and Table 3.2-4 for water and Castrol oil respectively.

Table 3.2-3:Contact angle calculation of for different surface roughness (Water).

Roughness(μm)	Contact Angle 1	Contact Angle 2	Average
0.220	88.82 °	88.07 °	88.45 °
0.359	83.94 °	83.64 °	83.79 °
0.434	80.93 °	80.58 °	80.75 °
0.47	77.47 °	77.09 °	77.28 °
0.499	75.66 °	74.48 °	75.07 °
0.559	74.47 °	73.21 °	73.84 °
0.59	68.73 °	68.95 °	68.84 °

Table 3.2-4:Contact angle calculation for different surface roughness (Castrol Oil).

Roughness(μm)	Contact Angle 1	Contact Angle 2	Average
0.220	37.49 °	48.71 °	43.10 °
0.359	45.00 °	37.75 °	41.38 °
0.434	35.54 °	45.00 °	40.27 °
0.470	40.40 °	37.65 °	39.03 °
0.499	39.96 °	37.29 °	38.63 °
0.559	38.74 °	31.53 °	35.14 °
0.590	29.62 °	28.52 °	29.07 °

In order to study the change in contact angle with time, after the drop is fully dispensed from the syringe, each drop's image is captured at every 1-second interval and contact angle at each time for different surfaces are determined. Table 3.2-5 and Table 3.2-6 shows the contact angle value for water and Castrol oil for different surface roughness in different time intervals. First of all, a horizontal line is sketched on the base of a liquid drop and two tangent lines are sketched on the

curve formed by liquid drop with a baseline to determine the contact angle (*Refers to Figures 3.2-1 and 3.2-2*). After the measurement of two contact angle form on the drop, the overall contact angle form is considered as taking the average between two angles. It is very difficult to get the exact contact angle of a liquid drop because it is almost difficult to draw perfect tangent in a curve, where the slight change in tangent line makes large different in contact angle.

During the experiment, it is difficult to dispense the same amount of liquid drops every time manually, so this may vary in contact angle value for same liquid and surfaces. The first drop of liquid on the surface of specimen is considered as initial drop shape (used to calculated first contact angle of the drop as 0 sec presented on Table 3.2-5) and contact angle after every one second are calculated for each specimen. This is done because in real life applications we can see the liquid for a longer period of time in the device. We can see contact angle changes with every second and becomes constant after a longer time.

Table 3.2-5:Contact angle calculation for different surface roughness w.r.t to time (Water).

	Surface Roughness(μm)							
Time(Seconds)		0.220	0.359	0.434	0.470	0.499	0.559	0.590
0	Average Contact Angle (Degree)	88.44 °	83.79 °	80.75 °	77.28 °	75.07 °	73.84 °	68.84 °
1		80.12 °	75.77 °	78.88 °	74.22 °	74.75 °	70.86 °	66.88 °
2		79.89 °	73.26 °	76.32 °	73.89 °	73.55 °	70.55 °	66.12 °
3		78.34 °	73.11 °	76.24 °	73.54 °	72.11 °	69.25 °	66.00 °
4		78.24 °	73.01 °	76.22 °	72.75 °	72.10 °	69.22 °	65.85 °
5		78.24 °	72.80 °	76.12 °	72.55 °	72.10 °	69.22 °	64.45 °
6		79.51 °	72.80 °	75.11 °	72.51 °	72.10 °	69.18 °	64.20 °

Table 3.2-6:Contact angle calculation for different surface roughness w.r.t to time (Castrol Oil).

		Surface Roughness(μm)						
Time(Seconds)		0.220	0.36	0.434	0.470	0.499	0.559	0.590
0	Average Contact Angle (Degree)	43.10°	41.38°	40.27°	39.03°	38.63°	35.14°	29.07°
1		34.76°	30.36°	32.81°	35.43°	31.09°	32.14°	27.62°
2		33.84°	24.24°	30.65°	33.02°	30.55°	28.47°	25.67°
3		33.11°	23.64°	29.09°	30.86°	27.59°	27.73°	25.27°
4		28.69°	22.39°	24.53°	29.54°	26.36°	24.34°	24.19°
5		26.94°	20.75°	23.32°	26.08°	24.46°	23.31°	22.27°
6		26.11°	18.38°	21.99°	24.99°	23.94°	22.90°	21.67°

Figures 3.2-1 and 3.2-2 show the determination of contact angle of water and Castrol oil drops. From the result, it is determined that, for same surface roughness, water drop have a higher contact angle than the Castrol oil. For same time interval increase, there is a more decrease in contact angle for Castrol oil than water. The relationship between surface roughness and the contact angle is presented on Figure 3.2-3 below. It is found that surface roughness has a significant effect on contact angle, contact angle decreases with increase in mean surface roughness. Castrol oil has a lower contact angle value than water for same surface roughness. This is because as we know when surface tension reduces, droplets tends to spreads and contact angle decreases, where the surface tension of water (0.072N/m) is higher than the Castrol oil (0.035N/m) at room temperature.

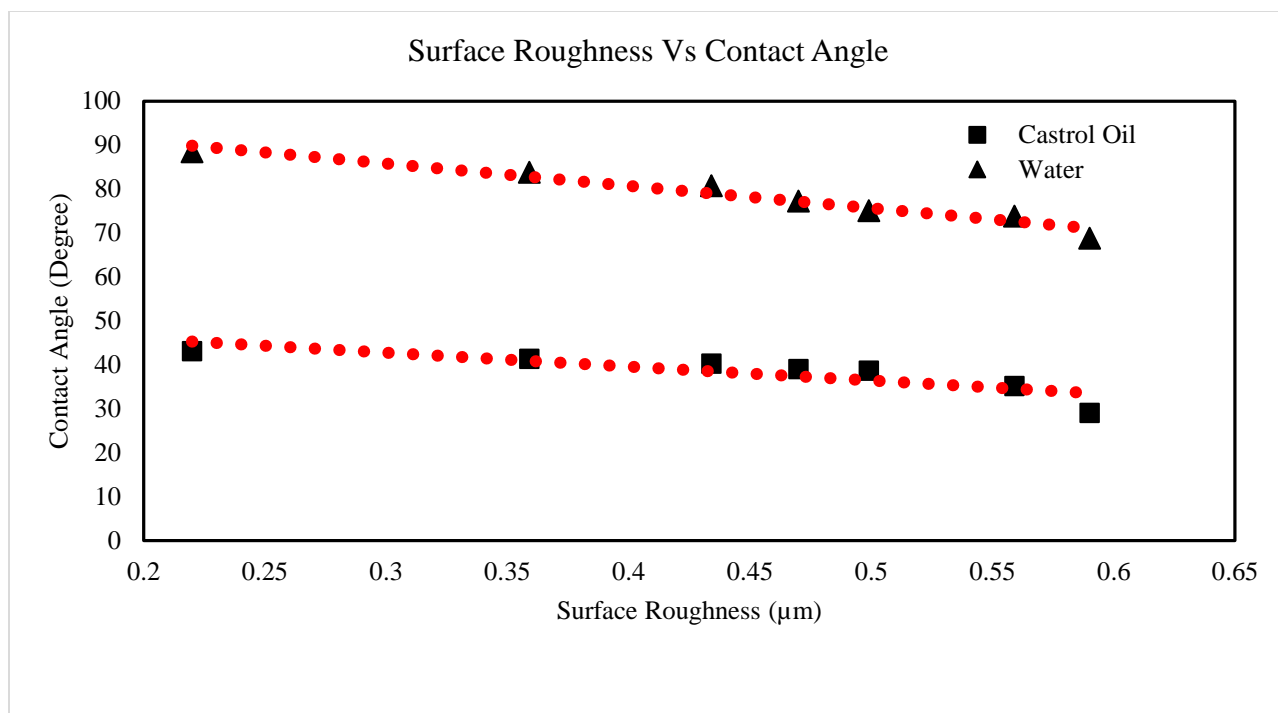


Figure 3.2-3: Relationship between surface roughness and contact angle for water and Castrol oil.

Liquid-mediated contact separation is performed for water drop and Castrol oil which is present on Figures 3.2-4 and 3.2-5. Initially, liquid drop with a certain value (0.013ml for water and 0.0105ml for Castrol oil) is inserted on lower surface from vertically projected syringe. After dispensing of drop on the surface, another surface is brought closer in order to make liquid mediated contact separation for flat on flat solid surfaces. Formation of menisci during the contact separation is shown in Figures 3.2-4 and 3.2-4. It is found that Castrol oil drop spread rapidly than the water drop. And when the surfaces bring to separate, menisci formed by water break quickly than the Castrol oil. We can also do the contact angle analysis during the separation as well, by considering the different factors.

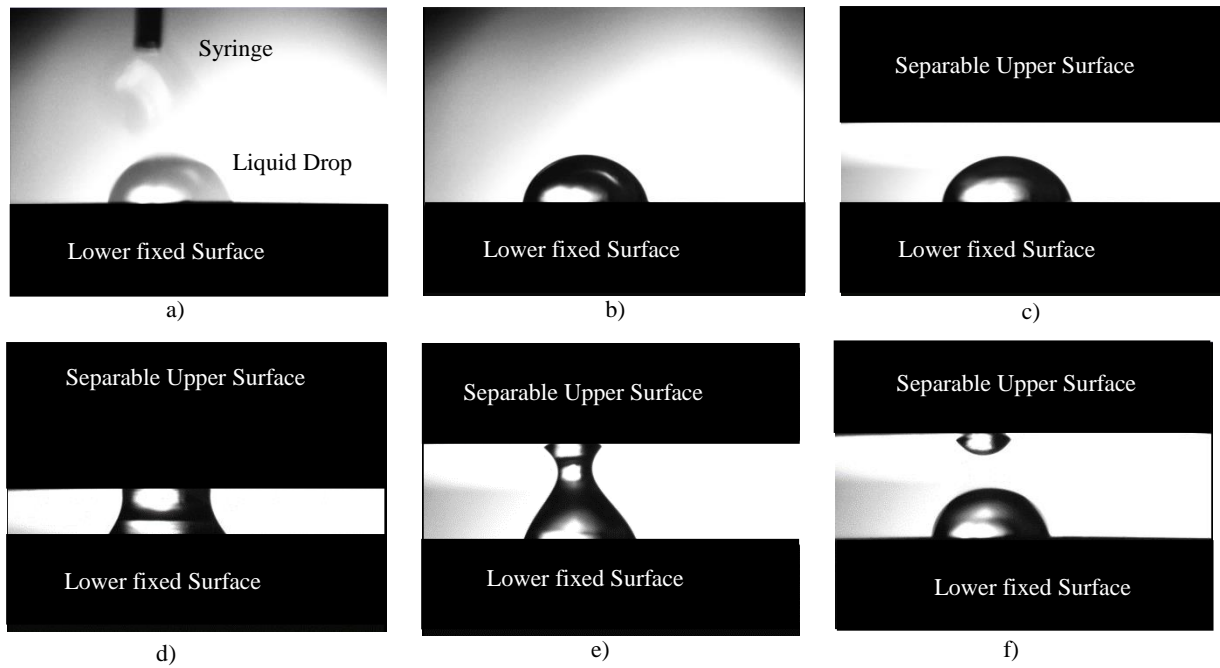


Figure 3.2-1: Illustration of different contacts angle during liquid mediated contact separation (600 Grit, water).

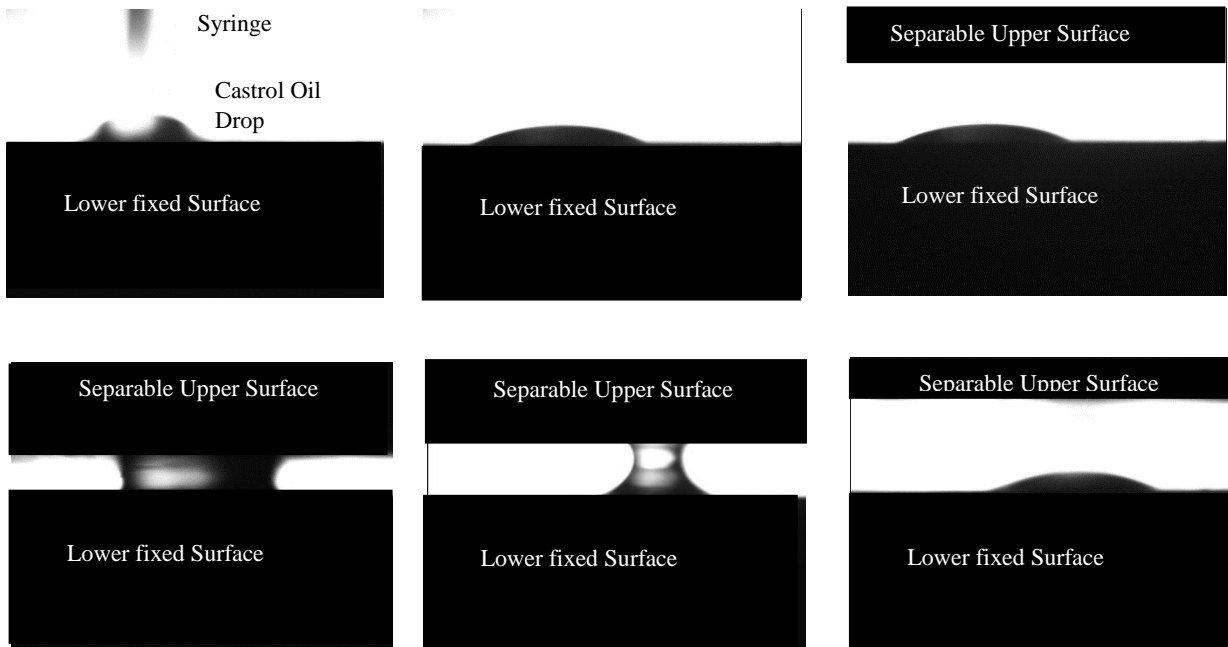


Figure 3.2-5: Illustration of different contacts angle during liquid mediated contact separation (600 Grit, Castrol oil).

In every step show in Figures 3.2-4 and 3.2-5, we can determine the contact angle of liquid drop before and after the separation made for same surface roughness surfaces as well. In order to perform the numerical modeling simulation to analysis the role of meniscus and viscous force, we assume that the formed meniscus as arc shaped which is confirmed form the observation above figure 3.2-4 and 3.2-5. When the separation is made, there is a change in the meniscus area with the change in the separation height. The change is the meniscus neck radius is different for different liquid properties (water and Castrol oil as different liquid properties).

3.3 APPLICATIONS

Many devices like magnetic head disks interface, digital micro-mirror devices, and diesel fuel injectors etc. experience adhesion/friction/stiction problems due to start –stop operation, physical contact, sliding phenomenon, which generates friction. Protective diamond-like carbon (DLC) coating with a thin lubricant overlay is used to provide low friction, low wear, and corrosion resistance. Due to these, meniscus and viscous forces involved in the separation operation need to be addressed to resolve the potential problems like adhesion/friction/stiction [5].

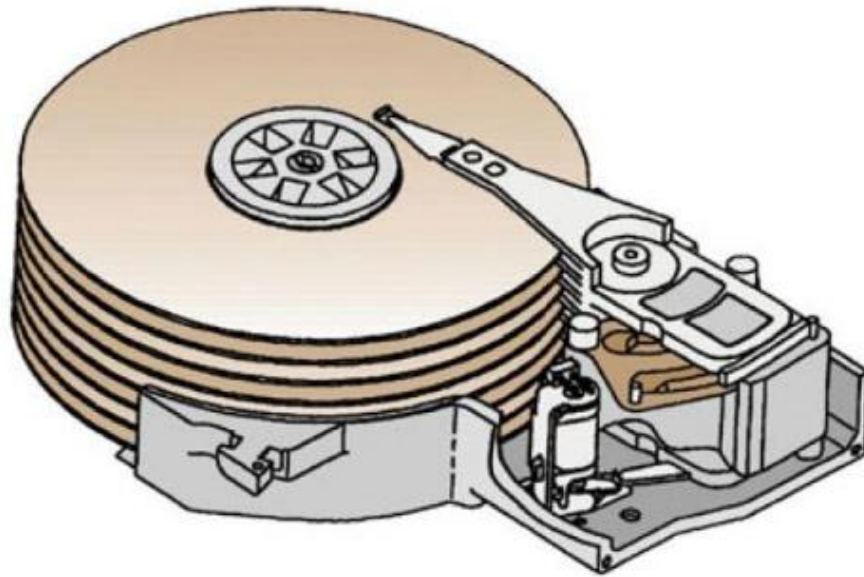


Figure 3.3-1: Schematic of a data processing magnetic rigid disk drive [21].

Since a larger contact angle and lower surface energy lead to a smaller meniscus force, coating the surfaces with a material with a lower surface energy and larger contact angle can also help to reduce the resultant adhesive force. The amount of liquid at contacting interface can be reduced to mitigate meniscus and viscous force. Heating the liquid just before relative motion reduces the viscosity of the liquid and can help to achieve lower viscous force [21].

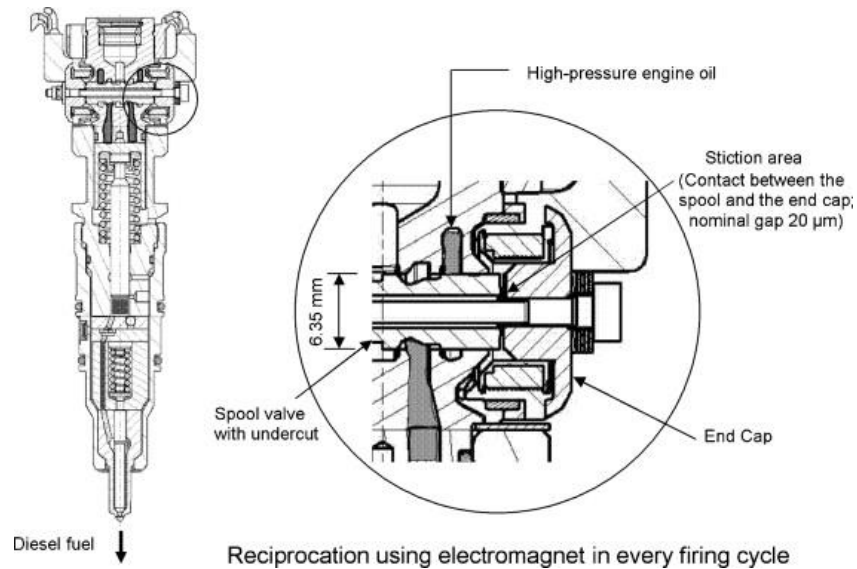


Figure 3.3-2: Schematic of diesel fuel injector which experiences adhesion [5].

Fuel injectors are a typical example of macro-scale devices with high stiction due to the thin liquid film shown in Figure 3.3-2. During the process, high-pressure engine oil comes in and pushes a piston to move downward to push the diesel fuel to inject into the engine. The intake of the high-pressure engine oil is controlled by the reciprocating motion of a spool valve, realized by the applied electromagnet attached at the end of an end cap. Adhesion occurs frequently between the spool valve and the end. This situation is even worse in cold weather. The adhesion problem reduces the reliability of the device. The solving of the problem needs to be based on the understanding of the forces involved during separation of two solid surfaces from the thin liquid film [5].

We can also use the result (*Figures 3.1-1 to 3.1-8*) from numerical modelling simulation analysis as the liquid properties selection model chart for a specific critical meniscus area and separation height used for the micro-nano device applications describe as above.

3.4 CONCLUSION AND SUGGESTION FOR FUTURE WORKS

Both meniscus and viscous forces are significantly affected by surface contact parameters such as contact angle, initial separation height, surface tension and liquid viscosity. Both forces can be a dominant force depending on the size of the meniscus area. The analysis shows that critical meniscus area at which meniscus and viscous force change the roles during flat on flat liquid-mediated contact separation depends upon contact configuration such as viscosity, surface tension, and separation height. For the same separation time, initial meniscus height, change in viscosity and surface tension of the liquid have a significant effect on the critical meniscus area. Critical meniscus area decreases with higher slope (rate of change of critical meniscus area) for the higher separation height (i.e. = 6nm) and followed by decreasing initial separation (5nm, 4nm, 3nm, and 2nm). Also, it is observed that critical meniscus area moves to a smaller value with the increase in viscosity. The change in the critical meniscus area from 2nm to 6nm initial separation height is almost constant as viscosity increases. With the increase in surface tension value, critical meniscus area increases and also changes in critical meniscus area from 2nm to 6nm initial separation is always constant. When either viscosity or surface tension increases, critical meniscus area always increases with increase in initial separation. The increase or decrease in the meniscus and viscous forces during liquid-mediated contact separation are significantly affected by the change in meniscus area. The two types of forces are comparable when the critical meniscus area is reached. The domination of either meniscus force or viscous force occurs with the larger or smaller value of critical meniscus area.

The studies show that both meniscus force and viscous force are largely dependent on the separation distance. Both forces exhibit a rapid changing rate at the beginning. Meniscus force

decreases with separation while viscous force has an opposite trend. The value of initial separation plays an important role affecting the break point and the magnitudes of the two forces. Meniscus area significantly affects the magnitudes of the meniscus and viscous forces. Viscous force increases (with an increase in meniscus area) much faster as compared to meniscus force. The increase or decrease in the meniscus area can change the roles of these two types of forces. For a fixed separation time t_s , the two types of forces are comparable when a critical meniscus area is reached. Larger or smaller value of the meniscus area leads to either viscous or meniscus force to be the dominant force of the system. Initial meniscus height affects the role of the meniscus and viscous forces. The increase in the meniscus height leads to both meniscus force and viscous force decrease. Viscous force becomes dominant at relatively larger meniscus area when the initial meniscus height is larger. Critical meniscus area (at which meniscus and viscous forces switch roles) changes with not only the initial meniscus height but also the liquid properties. Initially lower meniscus height with larger liquid viscosity leads to smaller critical meniscus area. Thus, the viscous force can be a dominant force even though the liquid meniscus is very small. When control of interfacial adhesion (due to liquid mediates contacting solid surfaces) is needed, the roles of the involved meniscus and viscous forces need to be determined. To effectively control the adhesion, the factors such as the initial separation height (of the two surfaces), the type of liquid, the formed meniscus area etc. all need to be considered. And the experimental analysis shows that the surface roughness has a significant effect on contact angle. Liquid drops with higher surface tension always tend to smaller.

Many assumptions are considered for flat on flat liquid mediated contact separation analysis in this work. All the assumptions that are considered during this research may not occur in real life application all the time. In further studies, It would be of interest to analyze meniscus and viscous

force with consideration of with free boundary separation, the air inside the meniscus and consideration of gravitation as usually occurs in real world applications. It would be interesting if the analytically investigated data verified with experiments. Two surfaces with same surface roughness can be made to perform the liquid mediated contact separation. Contact angle and the meniscus shape can be examined. All this analysis can also be performed for flat on sphere and sphere on sphere contact separation.

4 BIBLIOGRAPHY

- [1] H. W. Kang, H. J. Sung, T. M. Lee and C. J. Kim, "Liquid Transfer between Two Separating Plates for Micro-gravureoffset Printing," *Micromech. Microeng.*, p. 19, 2009.
- [2] S. Cai and B. Bhushan, "Meniscus and Viscous Forces during Separation of Hydrophilic and Hydrophobic Smooth/Rough Surfaces with Symmetric and Asymmetric Contact Angles," *Philosophical Transactions of the Royal Society :A Mathematical,Physical and Engineering Sciences*, 2008b.
- [3] S. Liu, C. Zhang and H. Zhang, "Meniscus and Viscous Forces during the Nanoscale Separation of Sphere-on-sphere Contact Surfaces," *Advanced Material Research*, Vols. 199-200, pp. 739-744, 21 02 2011.
- [4] S. Cai and B. Bhushan, "Meniscus and Viscous forces during normal separation of liquid-mediated contacts," 2007.
- [5] S. Cai and B. Bhushan, "Meniscus and viscous forces during separation of hydrophilic and hydrophobic surfaces with liquid-mediated contacts.," in *Materials Science and Engineering R report*, 2008a.
- [6] S. Cai, Y. Zhao and B. Bhushan, "Dry and wet contact analyses for the study of friction and wear trends," *In Society of Tribologists and Lubrication Engineers Annual Meeting and Exhibition R-reports*, pp. 326-328, 2009.
- [7] B. Bhushan, *Introduction to Tribology*, A John Wiley and Sons ,Publications, 2013.

- [8] B. Bhushan, "Tribology and Mechanics of Magnetic Storage Devices," *Springer*, 1996.
- [9] B. Bhushan, Principles and Applications of Tribology, A Wiley-Interscience Publication, 1999.
- [10] B. Bhushan, "Adhesion and Stiction : Mechanisms, measurement techniques , and methods for reduction," *Nanotribology Laboratory for Information Storage and MEMS/NEMS , The Ohio State University*, 2003.
- [11] A. T. Kittu, R. Bulut and J. Puckette, "Effects of surface roughness on contact angle measurements on a limestone aggregate," *Recent Development in Vaaluation of pavements and paving materials GSP 249 ASCE 2014*, 2014.
- [12] R. J. Good, M. K. Chaudhury and C. Yeung, "A new approach for determining roughness by means of contact angles on solids," *Department of Chemical Engineering, State University of NY at Buffalo, Buffalo, NY 14260, USA*, pp. 181-197, 1998.
- [13] H. Chen, A. Amirfazli and T. Tang, "Modeling Liquid Bridge between Surfaces with Contact Angle Hysteresis," *Langmuir*, pp. 3310-3319, 2013.
- [14] L. Wang, R. Weibin, G. Bin, H. Guiming and S. Lining, "Dynamic Separation of a Sphere from a Flat or Sphere in the Presence of a Liquid Meniscus.," *Tribology Transactions*, 2011.
- [15] V. Popov, "Contact mechanics and friction physical principles and applications," *Heidelberg:Springer*, 2010.

- [16] D. Bonn, J. Eggers, J. Indekeu, J. Meunier and E. Rolley, "Wetting and Spreading," *Rev.Mod.Phys*, pp. 739-805, 2009.
- [17] A. Colak, H. Wormeester, H. Zandvliet and B. Poelsema, "Surface adhesion and its dependence on surface roughness and humidity measured with a flat tip," *Applied Surface Science*, pp. 6938-6942, 2012.
- [18] S. Cai and B. Bhushan, "Viscous force during tangential separation of meniscus bridges," *Philosophical Magazine*, pp. 449-461, 2008.
- [19] P. Dhital, C. Shaobiao and Y. Zhao, "The Role of Adhesive Forces Due to Surface Separation from Liquid Menisci," *Society of Tribology Lubrication and Engineering 71st Annual Meeting*, 2016.
- [20] S. Cai, P. Dhital and Y. Zhao, "Interfacial Adhesion due to Liquid Mediated Contact of Hydrophilic Solid Surfaces," *International Conference on Structural, Mechanical and Materials Engineering (ICSMME 2015)*, 2015.
- [21] B. Bhushan, *Nanotribology and Nanomechanics I*, Springer, 2011.
- [22] F. M. Orr, L. E. Scriven and A. P. Rivas, in *J.Fluid Mech*, 1975, pp. 723-742.